

# Solubility and Diffusion of H<sub>2</sub>S and CO<sub>2</sub> in the Ionic Liquid 1-(2-Hydroxyethyl)-3-methylimidazolium Tetrafluoroborate

Mohammad Shokouhi, Mina Adibi, Amir Hossein Jalili,\* Masih Hosseini-Jenab, and Ali Mehdizadeh

Gas Science Department, Research Institute of Petroleum Industry (RIPI), National Iranian Oil Company (NIOC), P.O. Box 14665-137, West Blvd. Azadi Sports Complex, Tehran, Iran

The solubilities and diffusion coefficients of hydrogen sulfide and carbon dioxide gases in the ionic liquid (IL) 1-(2-hydroxyethyl)-3-methylimidazolium tetrafluoroborate ([hemim][BF<sub>4</sub>]), at temperatures ranging from (303.15 to 353.15) K and pressures up to 1.1 MPa, were determined. The solubility data were correlated using the Krichevsky–Kasarnovsky equation, and Henry's law constants at different temperatures were obtained. From the solubility data, the partial molar thermodynamic functions of solution such as Gibbs energy, enthalpy, and entropy were calculated. The diffusion coefficients were obtained for H<sub>2</sub>S and CO<sub>2</sub> using a semi-infinite volume approach, and a correlation equation with temperature is presented for each gas. A comparison showed that the solubility of H<sub>2</sub>S was about three times its magnitude, and its diffusion coefficient is of the same order of magnitude as that of CO<sub>2</sub> in the IL studied in this work.

## Introduction

The acid gases hydrogen sulfide and carbon dioxide are produced along with methane and light hydrocarbons in many oil and gas fields.<sup>1</sup> Alkanolamines, especially monoethanolamine, diethanolamine, and methyldiethanolamine, are the main constituents of aqueous solutions used in industrial natural gas treating plants.<sup>1</sup> There are some disadvantages in the commercial use of these alkanolamine solutions, including loss of the alkanolamine and transfer of water into the gas stream during the desorption stage and degradation of alkanolamines to form corrosive byproducts, which make the process economically expensive.<sup>2</sup>

Room-temperature ionic liquids (RTILs) are molten salts that are liquid over a wide temperature range including ambient temperatures.<sup>3</sup> Their most remarkable characteristic is that they have negligibly small vapor pressure, meaning that ionic liquids (ILs) are essentially nonvolatile, nonflammable, and odorless. They also have high thermal and electrochemical stability. Nowadays, one of the active research areas is to explore task-specific ILs<sup>4</sup> to replace conventional alkanolamine solutions for acid gases (CO<sub>2</sub> and H<sub>2</sub>S) removal in gas sweetening processes.

An important feature in the evaluation of ILs for potential use in industrial natural-gas treating processes is the knowledge of the solubility and the rate of solubility, that is, diffusion coefficients of gases at various temperatures and pressures. In the past few years, a growing number of measurements reporting the solubility and diffusion of CO<sub>2</sub> in various ILs have become available (see, for example, refs 5 to 10). However, experimental data for the solubility and diffusion of hydrogen sulfide in ILs are scarce. Jou and Mather<sup>11</sup> have reported the solubility of H<sub>2</sub>S in [bmim][PF<sub>6</sub>] at temperatures from (298.15 to 403.15) K and pressures up to 9.6 MPa. The solubility of H<sub>2</sub>S in different 1-butyl-3-methylimidazolium based ILs with different anions and in a series of bis(trifluoromethyl) sulfonylimide ILs with different cations at 298.15 K and 1400 kPa is reported by

Pomelli et al.<sup>12</sup> Jalili et al.<sup>13</sup> have reported the solubility of H<sub>2</sub>S in [bmim][PF<sub>6</sub>], [bmim][BF<sub>4</sub>], and [bmim][Tf<sub>2</sub>N] at temperatures ranging from (303.15 to 343.15) K and pressures up to 1 MPa. Subsequently, they reported<sup>14</sup> experimental data for the solubility of H<sub>2</sub>S in [hmim][PF<sub>6</sub>], [hmim][BF<sub>4</sub>], and [hmim][Tf<sub>2</sub>N] at temperatures ranging from (303.15 to 343.15) K and pressures up to 1.1 MPa. They have used the obtained data to estimate Henry's law constants and thermodynamic functions of solution at different temperatures.

This paper focuses on the solubility and diffusion coefficient of H<sub>2</sub>S and CO<sub>2</sub> in the IL ([hemim][BF<sub>4</sub>]) at six temperatures from (303.15 to 353.15) K. The solubilities determined were used to estimate Henry's law constants and partial molar thermodynamic functions of solution of H<sub>2</sub>S and CO<sub>2</sub> at different temperatures. A correlation equation for the obtained solubility, diffusion, and partial molar volume at infinite dilution data of each gas with temperature is presented here. The density of the IL considered in this work is also reported at six temperatures from (300.71 to 314.35) K.

## Experimental Section

**Materials.** Carbon dioxide and hydrogen sulfide (c.p. grade 99.5 % min) were obtained from Roham Gas Company.

The IL [hemim][BF<sub>4</sub>] was prepared according to the synthesis method described by Yeon et al.<sup>15</sup> and Dubreuil and Bazureau.<sup>16</sup>

A portion of 13.9 g (0.169 mol) of 1-methylimidazole (Merck, 99 %), distilled over KOH, was added slowly to 15.0 g (0.186 mol) of freshly distilled 2-chloroethanol in a round-bottomed flask equipped with a magnetic stirrer and a condenser under nitrogen atmosphere. Then, the mixture was refluxed at 373 K for 4 h. After cooling to 343 K, the reaction mixture was washed four times using 20 % of its weight of ethyl acetate. The product was dried in vacuo at 343 K for 8 h. The product, 1-(2-hydroxyethyl)-3-methylimidazolium chloride ([hemim][Cl]), was obtained as a white crystalline solid (17.9 g, 65 % yield). <sup>1</sup>H NMR (500 MHz, D<sub>2</sub>O, 25 °C): δ (ppm) = 3.87 (3H, s, NCH<sub>3</sub>), 3.89 (2H, t, NCH<sub>2</sub>CH<sub>2</sub>OH), 4.28 (2H, t, NCH<sub>2</sub>CH<sub>2</sub>OH), 7.42 (1H, d, H-4), 7.47 (1H, d, H-5), 8.71 (1H, s, H-2).

\* To whom correspondence should be addressed. E-mail: jaliliah@ripi.ir. Tel./fax: 98-21-44739716.

A portion of 30.0 g (0.185 mol) of [hemim][Cl] was reacted with 26.4 g (0.24 mol) of sodium tetrafluoroborate (NaBF<sub>4</sub>) in acetonitrile solvent under nitrogen atmosphere at room temperature for 48 h. The reaction mixture was cooled to 255 K overnight and then filtered through a short column of Celite to remove NaCl. The solvent was removed using a rotary evaporator, and the residual chloride (AgNO<sub>3</sub>) test performed on product was negative. The product, 1-(2-hydroxyethyl)-3-methylimidazolium tetrafluoroborate ([hemim][BF<sub>4</sub>]), was obtained as a viscous material (62 % yield). Karl Fischer test showing < 100 ppm of water and the absence of chloride ion confirmed the product purity (> 99.5 %). <sup>1</sup>H NMR (500 MHz, D<sub>2</sub>O, 25 °C): δ (ppm) = 3.83 (3H, s, NCH<sub>3</sub>), 3.87 (2H, t, NCH<sub>2</sub>CH<sub>2</sub>OH), 4.24 (2H, t, NCH<sub>2</sub>CH<sub>2</sub>OH), 7.38 (1H, d, H-4), 7.43 (1H, d, H-5), 8.66 (1H, s, H-2).

**Apparatus and Procedure.** The details of the experimental method for the measurement of gas solubility have previously been presented,<sup>13</sup> and only a short description will be provided here. In this technique, a known quantity of gaseous solute is contacted with a known quantity of degassed solvent at a constant temperature inside an equilibrium cell of known volume. When the thermodynamic equilibrium is reached, the pressure above the liquid solution is constant and directly related to the solubility of the gas in the liquid. The amount of solute present in the liquid solution,  $n_{\text{solute}}^l$ , is calculated by the difference between two PVT measurements: first, when the gas is introduced from the gas container of known volume into the equilibrium cell containing the IL, and second, after thermodynamic equilibrium is reached (i.e., pressure of the autoclave remains constant and no longer changes with time):

$$n_{\text{solute}}^l = n_{\text{total}} - n_{\text{solute}}^g \quad (1)$$

where  $n_{\text{total}}$  is the total number of moles of gas (in this case H<sub>2</sub>S or CO<sub>2</sub>) injected from the gas container into the autoclave and calculated using the following equation:

$$n_{\text{total}} = \frac{V_{\text{gc}}}{RT_{\text{gc}}} \left( \frac{P_i}{Z_i} - \frac{P_f}{Z_f} \right) \quad (2)$$

where  $V_{\text{gc}}$  denotes the volume of the gas container,  $Z_i$  and  $Z_f$  are the compressibility factors corresponding to the initial and final pressures  $P_i$  and  $P_f$ , respectively, in the gas container before and after transferring the gas, and  $T_{\text{gc}}$  is the temperature of the gas container. Compressibility factors were calculated using the most accurate PVT data presented by the National Institute of Standards and Technology (NIST) for pure compounds.<sup>17</sup>  $n_{\text{solute}}^g$  in eq 1 is the number of moles of gas solute left in the gas phase and was determined from the following equation:

$$n_{\text{solute}}^g = \frac{V_{\text{g}} P}{ZRT} \quad (3)$$

where  $V_{\text{g}}$  is the volume of the gas-phase above the IL phase,  $T$  is the equilibrium temperature of the cell, and  $Z$  is the compressibility factor of gas solute at  $P$  and  $T$ . In all experiments, before solubility measurements, the IL was dried in vacuo (below 1.0 kPa) for about 48 h at a temperature of 343 K to remove trace amounts of moisture and volatile impurities. The water content of ILs was found to be below  $100 \pm 10$  ppm by a Mettler model DL-37 Karl Fischer volumetric titrator. The temperature of the equilibrium cell, which was placed inside of a water recirculation bath (Haake, model D8), was measured with a Lutron model TM-917 digital thermometer with a 0.01 K resolution using a Pt-100 sensor inserted into the cell. The pressure of the equilibrium cell was measured using a BD model

D95199 pressure transmitter sensor in the range of (0 to 1) MPa, and that of the gas container was measured using a Druck model PTX 1400 pressure transmitter sensor in the range of (0 to 4) MPa. The pressure sensors were calibrated against a dead-weight gauge and were uncertain to within 0.1 % of full scale.

The diffusion coefficient for the diffusivity of H<sub>2</sub>S and CO<sub>2</sub> gases into [hemim][BF<sub>4</sub>] was measured by the apparatus used in this work for measuring gas solubilities and the method devised by Camper et al.<sup>6</sup> This way, the diffusion measurements were made through the measurement of pressure with respect to time during the first 20 min in which the magnetic stirrer was turned off so that there was a stagnant layer of IL. Some time after 20 min, the stirrer was turned on so that the time needed to reach equilibrium would be significantly reduced. This method is based on a semi-infinite diffusion model, which is developed mathematically by Crank.<sup>18</sup> The equations needed for the measurement of diffusion coefficients are introduced below.

The concentration at point  $x$  below the surface of a fluid at time  $t$  is defined by<sup>18</sup>

$$C = C_{x=t=0} \operatorname{erfc} \frac{x}{2\sqrt{Dt}} + k\sqrt{\pi t} \left[ \operatorname{ierfc} \left( \frac{x}{2\sqrt{Dt}} \right) \right] \quad (4)$$

where  $C_{x=t=0}$  is the surface concentration at time  $t = 0$ , which is related to surface concentration by eq 5

$$C_{x=0} = C_{x=t=0} + k\sqrt{t} \quad (5)$$

$D$  is the diffusion coefficient. The rate of gain of the diffusing gas into the semi-infinite volume is defined by<sup>18</sup>

$$\left( D \frac{\partial C}{\partial x} \right)_{x=0} = C_{x=t=0} \frac{1}{\sqrt{Dt\pi}} - \frac{\sqrt{\pi}}{2\sqrt{D}} k \quad (6)$$

From eq 6, the cumulative gas that has diffused into the semi-infinite volume at time  $t$  is found using eq 7.<sup>18</sup>

$$M_t = \int_0^t \left( D \frac{\partial C}{\partial x} \right)_{x=0} dt = \sqrt{D} \left[ 2C_{x=t=0} \sqrt{\frac{t}{\pi}} - \frac{1}{2} k t \sqrt{\pi} \right] = \sqrt{D} \varepsilon \quad (7)$$

The following assumptions were implicitly made while using the semi-infinite volume approach. (1) Concentration does not vary radially. (2) The volume is considered infinite in the  $x > 0$  direction, where  $x = 0$  at the surface of the IL, for the time interval used in determining the diffusion coefficient. (3) Joule–Thomson effects are negligible for the time interval used in determining the diffusion coefficient. (4) The surface concentration at  $x = 0$  and  $t > 2$  min is at equilibrium with the gas. Time intervals greater than 2 min were used so that any surface adsorption that is not in equilibrium with the gas would not affect the values obtained for the diffusion coefficients. Assumption 1 is naturally valid because the autoclave is a regular cylinder with a uniform circular cross section and also there is no mechanical agitation disturbing the stagnant liquid during diffusion measurement. The validity of assumption 2 was checked mathematically for the two systems studied in this work using eq 4 to determine the concentration of the solute at the bottom of the autoclave at the final diffusion time. The solute concentration at the bottom of the autoclave was the highest for CO<sub>2</sub> at 80 °C, where the ratio of the initial surface concentration to the concentration at the bottom of the autoclave was < 0.15 %. The validity of assumption 3 has previously been checked experimentally by Camper et al.<sup>6</sup> Given that the temperature of the gas before injection is the same as that of the autoclave and thus cooling of the gas is minimum due to

**Table 1. Mole Fraction Solubility of Hydrogen Sulfide Gas,  $x$ , in [hemim][BF<sub>4</sub>]**

$p/\text{kPa}$	$x$	$p/\text{kPa}$	$x$	$p/\text{kPa}$	$x$
$T/\text{K} = 303.15$		$T/\text{K} = 313.15$		$T/\text{K} = 323.15$	
136	$0.039 \pm 0.001$	121	$0.028 \pm 0.001$	142	$0.026 \pm 0.001$
164	$0.048 \pm 0.001$	235	$0.055 \pm 0.001$	250	$0.047 \pm 0.001$
289	$0.081 \pm 0.001$	338	$0.076 \pm 0.001$	350	$0.065 \pm 0.001$
462	$0.126 \pm 0.001$	505	$0.112 \pm 0.001$	444	$0.083 \pm 0.001$
532	$0.144 \pm 0.001$	641	$0.140 \pm 0.001$	531	$0.097 \pm 0.001$
652	$0.174 \pm 0.002$	760	$0.162 \pm 0.001$	606	$0.111 \pm 0.001$
703	$0.187 \pm 0.003$	890	$0.186 \pm 0.001$	675	$0.123 \pm 0.001$
802	$0.208 \pm 0.004$	969	$0.202 \pm 0.002$	793	$0.142 \pm 0.001$
969	$0.235 \pm 0.004$	1066	$0.217 \pm 0.001$	931	$0.164 \pm 0.001$
1027	$0.247 \pm 0.002$			1003	$0.176 \pm 0.002$
$T/\text{K} = 333.15$		$T/\text{K} = 343.15$		$T/\text{K} = 353.15$	
155	$0.025 \pm 0.001$	300	$0.041 \pm 0.001$	165	$0.020 \pm 0.001$
277	$0.045 \pm 0.001$	408	$0.055 \pm 0.001$	318	$0.039 \pm 0.001$
394	$0.062 \pm 0.001$	518	$0.070 \pm 0.001$	442	$0.055 \pm 0.001$
495	$0.077 \pm 0.001$	613	$0.082 \pm 0.001$	644	$0.079 \pm 0.001$
613	$0.096 \pm 0.002$	755	$0.099 \pm 0.001$	845	$0.102 \pm 0.002$
757	$0.116 \pm 0.002$	872	$0.115 \pm 0.002$	964	$0.115 \pm 0.002$
868	$0.133 \pm 0.002$	989	$0.127 \pm 0.002$	1047	$0.126 \pm 0.002$
		1066	$0.137 \pm 0.003$		

**Table 2. Mole Fraction Solubility of Carbon Dioxide Gas,  $x$ , in [hemim][BF<sub>4</sub>]**

$p/\text{kPa}$	$x$	$p/\text{kPa}$	$x$	$p/\text{kPa}$	$x$
$T/\text{K} = 303.15$		$T/\text{K} = 313.15$		$T/\text{K} = 323.15$	
175	$0.018 \pm 0.001$	114	$0.008 \pm 0.001$	119	$0.007 \pm 0.001$
233	$0.021 \pm 0.001$	291	$0.019 \pm 0.001$	300	$0.019 \pm 0.001$
350	$0.033 \pm 0.001$	408	$0.031 \pm 0.001$	427	$0.028 \pm 0.001$
434	$0.041 \pm 0.002$	549	$0.043 \pm 0.001$	571	$0.041 \pm 0.001$
645	$0.061 \pm 0.002$	677	$0.053 \pm 0.002$	846	$0.059 \pm 0.002$
733	$0.068 \pm 0.002$	808	$0.065 \pm 0.002$	960	$0.065 \pm 0.002$
766	$0.071 \pm 0.003$	917	$0.071 \pm 0.002$	1064	$0.072 \pm 0.002$
1102	$0.102 \pm 0.003$	1016	$0.079 \pm 0.003$		
$T/\text{K} = 333.15$		$T/\text{K} = 343.15$		$T/\text{K} = 353.15$	
125	$0.006 \pm 0.001$	130	$0.005 \pm 0.001$	135	$0.004 \pm 0.001$
312	$0.018 \pm 0.001$	325	$0.016 \pm 0.001$	335	$0.016 \pm 0.001$
444	$0.026 \pm 0.001$	460	$0.025 \pm 0.001$	479	$0.022 \pm 0.001$
597	$0.037 \pm 0.002$	619	$0.035 \pm 0.001$	644	$0.032 \pm 0.002$
738	$0.045 \pm 0.002$	768	$0.042 \pm 0.002$	796	$0.040 \pm 0.002$
882	$0.055 \pm 0.002$	917	$0.051 \pm 0.002$	950	$0.049 \pm 0.002$
999	$0.061 \pm 0.003$	1040	$0.057 \pm 0.003$	1194	$0.061 \pm 0.003$

Joule–Thomson expansion, this was considered a valid assumption here, too. In assumption 4 the nonequilibrium surface adsorption is omitted from our calculations where it gives rise to great uncertainties and has the greatest effect for the time intervals, which immediately follow the opening of the valve. The time required for  $C_{i=0}$  to first be in equilibrium with the gas was obtained from careful examination of Figures 2 and 3 where there is good linear correlation among the data points. The estimated overall uncertainty due to the above assumptions does not exceed  $\pm 5\%$ .

## Results and Discussion

The results of the measurement of the solubility of hydrogen sulfide and carbon dioxide in the IL [hemim][BF<sub>4</sub>] at temperatures of (303.15, 313.15, 323.15, 333.15, 343.15, and 353.15) K and pressures up to about 1 MPa are summarized in Tables 1 and 2. The reliability and accuracy of the method of measurement have been checked in our previous work.<sup>13</sup> The Krichevsky–Kasarnovsky equation<sup>12</sup> was used to model the experimental data obtained in this work:

$$\ln\left(\frac{f_2}{x_2}\right) = \ln K_h + \frac{V_2^\infty(P - P_1^s)}{RT} \quad (8)$$

where  $f_2$  is the fugacity of solute (hydrogen sulfide or carbon dioxide) in the gas phase,  $x_2$  is the mole fraction of solute in

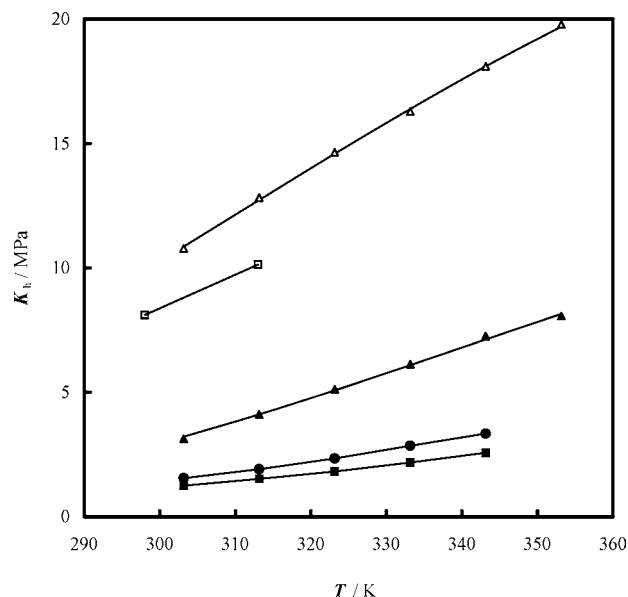


**Figure 1.** Comparison between Henry's law constants as a function of temperature for the solubility of H<sub>2</sub>S and CO<sub>2</sub> in [hemim][BF<sub>4</sub>] and [emim][BF<sub>4</sub>]: ▲, H<sub>2</sub>S in [hemim][BF<sub>4</sub>]; ●, H<sub>2</sub>S in [bmim][BF<sub>4</sub>] (ref 13); ■, H<sub>2</sub>S in [hmim][BF<sub>4</sub>] (ref 14); △, CO<sub>2</sub> in [hemim][BF<sub>4</sub>]; □, CO<sub>2</sub> in [emim][BF<sub>4</sub>] (ref 19).

the solvent 1,  $P_1^s$  is the saturated vapor pressure of solvent 1,  $K_h$  is Henry's law constant of gas solute 2 in solvent 1 at the pressure  $P$ ,  $V_2^\infty$  is the partial molar volume of gas solute 2 at infinite dilution,  $R$  is the universal gas constant, and  $T$  is the absolute temperature. In this case the vapor pressure of the solvent, the IL, is negligible; the saturated vapor pressure  $P_1^s$  is zero, and  $f_2$  can be substituted by the fugacity of pure hydrogen sulfide or carbon dioxide gas,  $f_2^0$ . Equation 8 then can be turned to eq 9

$$\ln \frac{f_2^0}{x_2} = \ln K_h + \frac{V_2^\infty P}{RT} \quad (9)$$

The fugacities of hydrogen sulfide and carbon dioxide were calculated using the most accurate corresponding states used by NIST for pure compounds.<sup>17</sup> The intercept of Krichevsky–Kasarnovsky plots (that is, plots of  $\ln(f_2^0/x_2)$  vs  $P$ ) at each temperature,  $T$ , yields  $\ln K_h$  at the specified temperature. The Henry's law constants are given in Table 3 for the solubility of H<sub>2</sub>S and CO<sub>2</sub> in the IL studied in this work together with their standard deviations. The Henry's law constants were fit by the equation,

$$\ln(K_h/\text{MPa}) = \sum_{i=0}^2 A_i(T/\text{K})^{-i} \quad (10)$$

The parameters  $A_i$  of eq 10 obtained for H<sub>2</sub>S and CO<sub>2</sub> are summarized in Table 4. The Henry's law constants for these two gases, as a function of temperature, are compared with each other in Figure 1. It can be observed that the solubility of both gases in the IL decreases by increasing the temperature and hydrogen sulfide is about three times as soluble as carbon dioxide in the IL studied in this work. This later point has previously explained by Pomelli et al.<sup>12</sup> from molecular point of view using extensive quantum chemical calculations and also by Jalili et al.<sup>13</sup> by means of obtained experimental thermodynamic functions of solution. The solubility curves also indicate that the solubility of H<sub>2</sub>S and CO<sub>2</sub> in the IL studied in this work are typical of that of physical solvents,<sup>13</sup> therefore obeying the

**Table 3. Thermodynamic Properties of H<sub>2</sub>S and CO<sub>2</sub> in the [hemim][BF<sub>4</sub>]**

$T$ K	$K_h$ MPa	$V_2^\infty \cdot 10^6$ $\text{m}^3 \cdot \text{mol}^{-1}$	$\Delta_{\text{sol}} G^\infty$ $\text{kJ} \cdot \text{mol}^{-1}$	$\Delta_{\text{sol}} H^\infty$ $\text{kJ} \cdot \text{mol}^{-1}$	$\Delta_{\text{sol}} S^\infty$ $\text{J} \cdot \text{mol}^{-1} \cdot \text{K}^{-1}$	$D \cdot 10^{10}$ $\text{m}^2 \cdot \text{s}^{-1}$
H <sub>2</sub> S						
303.15	3.13 ± 0.01	778 ± 14	8.68	-22.9	-104	1.79 ± 0.03
313.15	4.11 ± 0.01	357 ± 16	9.67	-20.2	-95.2	2.15 ± 0.04
323.15	5.12 ± 0.03	164 ± 5	10.6	-17.5	-87.0	2.76 ± 0.13
333.15	6.13 ± 0.03	87.4 ± 5	11.4	-15.1	-79.5	3.24 ± 0.08
343.15	7.26 ± 0.05	53.5 ± 5	12.2	-12.8	-72.6	3.80 ± 0.04
353.15	7.95 ± 0.08	8.69 ± 3	12.9	-10.6	-66.4	4.41 ± 0.15
CO <sub>2</sub>						
303.15	10.8 ± 0.02	-116 ± 3	11.8	-13.4	-83.1	1.40 ± 0.05
313.15	12.8 ± 0.02	-105 ± 2	12.6	-12.2	-79.1	2.09 ± 0.11
323.15	14.7 ± 0.02	-98 ± 1	13.4	-11.0	-75.5	3.94 ± 0.20
333.15	16.3 ± 0.02	-93 ± 2	14.1	-9.93	-72.2	4.65 ± 0.10
343.15	18.1 ± 0.03	-85 ± 1	14.8	-8.92	-69.2	5.71 ± 0.09
353.15	19.8 ± 0.05	-81 ± 1	15.5	-7.96	-66.5	7.16 ± 0.18

**Table 4. Numerical Values of the Parameters of Equations 10, 12, and 16**

$A_0$	$A_1$	$A_2$	$B_0$	$B_1$	$B_2$	$C_0$	$C_1$	$C_2$
H <sub>2</sub> S								
-1.00319	3744.7	-935674	53048	-308.83	0.44952	42.2436	-0.29589	0.000536
CO <sub>2</sub>								
0.50660	2718.8	-651619	-915.84	4.3188	-0.00554	-19.1668	0.02921	0.000127

**Table 5. Density of [hemim][BF<sub>4</sub>] and [emim][BF<sub>4</sub>] as a Function of Temperature**

$T$ K	$\rho$ $\text{kg} \cdot \text{m}^{-3}$	$T$ K	$\rho$ $\text{kg} \cdot \text{m}^{-3}$	$T$ K	$\rho$ $\text{kg} \cdot \text{m}^{-3}$
[hemim][BF <sub>4</sub> ]	this work	[hemim][BF <sub>4</sub> ]	ref 22	[emim][BF <sub>4</sub> ]	ref 20
300.71	1384	298.15	1308.0	293.15	1305
303.35	1380	303.15	1304.7	303.15	1296
304.95	1379	308.15	1301.4	313.15	1288
307.31	1376	313.15	1296.1	323.15	1280
310.81	1373	318.15	1294.7	333.15	1272
314.35	1369	323.15	1291.5	343.15	1264
		328.15	1288.3		

Henry's law. Also variations with the temperature of the Henry's law constant for the solubility of CO<sub>2</sub> in the conventional IL, 1-ethyl-3-methylimidazolium tetrafluoroborate ([emim][BF<sub>4</sub>]),<sup>19</sup> and that of H<sub>2</sub>S in 1-butyl-3-methylimidazolium tetrafluoroborate ([bmim][BF<sub>4</sub>])<sup>13</sup> and 1-hexyl-3-methylimidazolium tetrafluoroborate ([hmim][BF<sub>4</sub>])<sup>14</sup> are shown in Figure 1. It can be seen that CO<sub>2</sub> is more soluble in [emim][BF<sub>4</sub>] than [hemim][BF<sub>4</sub>]. To explain the observed difference in solubility, we measured the density of pure [hemim][BF<sub>4</sub>] at six temperatures from (300.71 to 314.35) K by using a calibrated glass picnometer. The obtained densities are summarized in Table 5, which show a good linear correlation with temperature represented by eq 11

$$(\rho/\text{kg} \cdot \text{m}^{-3}) = -0.00106(T/\text{K}) + 1.703 \quad (11)$$

These values agree within 6 % of the values obtained by Restolho et al.<sup>22</sup> from (298.15 to 328.15) K (listed in Table 5 for ease of comparison). Also shown in Table 5 are the densities of [emim][BF<sub>4</sub>] at temperatures from (293.15 to 343.15) K.<sup>20</sup> Comparison of these data reveals that the density of [hemim][BF<sub>4</sub>] is higher than that of [emim][BF<sub>4</sub>]. This can be explained on the basis of the fact that the presence of a hydroxyl group attached to the alkyl chain in [hemim][BF<sub>4</sub>] gives rise to a stronger attraction between imidazolium cations and also between imidazolium cations and tetrafluoroborate anions via hydrogen bonding. The strong hydrogen bonding attraction causes the cationic and anionic molecular species to join more compactly together in [hemim][BF<sub>4</sub>] than the corresponding cations and anions in [emim][BF<sub>4</sub>], which causes the void

volume in [hemim][BF<sub>4</sub>] to be lower than that of [emim][BF<sub>4</sub>] and thus the density of [hemim][BF<sub>4</sub>] to be higher than [emim][BF<sub>4</sub>]. The lower void volume in [hemim][BF<sub>4</sub>] relative to [emim][BF<sub>4</sub>] may also be one of the important factors for the observed lower solubility of CO<sub>2</sub> in [hemim][BF<sub>4</sub>] relative to [emim][BF<sub>4</sub>]. This same reasoning may be used to describe the higher solubility of H<sub>2</sub>S (Figure 1) in the conventional ILs [bmim][BF<sub>4</sub>] and [hmim][BF<sub>4</sub>] relative to [hemim][BF<sub>4</sub>] as long as the densities of both of them are lower than that of [hemim][BF<sub>4</sub>]. We are studying these observations, from molecular point of view, for the solubility of CO<sub>2</sub> and H<sub>2</sub>S in functionalized ILs by using a molecular dynamics (MD) simulation and will present the results in the near future.

The slope of the Krichevsky–Kasarnovsky plots at each temperature,  $T$ , yields  $V_2^\infty$  at the specified temperature. The obtained experimental data of partial molar volumes of gas solutes, H<sub>2</sub>S and CO<sub>2</sub>, at infinite dilution,  $V_2^\infty$ , are presented in Table 3. They were correlated with temperature using the following simple quadratic formula

$$V_2^\infty/\text{m}^3 \cdot \text{mol}^{-1} = \sum_{i=0}^2 B_i(T/\text{K})^i \quad (12)$$

The obtained parameters  $B_i$  of eq 12 for H<sub>2</sub>S and CO<sub>2</sub> are summarized in Table 4. It can be observed from Table 3 that the  $V_2^\infty$  values decrease with temperature from (778 · 10<sup>-6</sup> to 8.7 · 10<sup>-6</sup>) m<sup>3</sup> · mol<sup>-1</sup> for H<sub>2</sub>S, but in the case of CO<sub>2</sub> they increase with temperature from (-116 · 10<sup>-6</sup> to -81 · 10<sup>-6</sup>) m<sup>3</sup> · mol<sup>-1</sup>.

The variation with temperature of the solubility of solute (H<sub>2</sub>S and CO<sub>2</sub>) studied, expressed in Henry's law constant, is directly related to the thermodynamic properties of solution which, in the case of gaseous solutes at low pressures, is practically identical to the thermodynamic properties of solution.<sup>21</sup> The Gibbs energy of solution, corresponding to the change in Gibbs energy when the solute is transferred at constant temperature from the pure perfect gas at the standard pressure to the standard state of infinite dilution of the solute in the solvent is given by:<sup>21</sup>

$$\Delta_{\text{sol}}G^{\infty} = RT \ln\left(\frac{K_h}{P^0}\right) \quad (13)$$

where  $P^0$  is the standard state pressure. The partial molar differences in enthalpy and entropy between the two states can be obtained by calculating the corresponding partial derivatives of the Gibbs energy with respect to temperature

$$\Delta_{\text{sol}}H^{\infty} = -T^2 \frac{\partial}{\partial T} \left( \frac{\Delta_{\text{sol}}G^{\infty}}{T} \right) = -RT^2 \frac{\partial}{\partial T} \left[ \ln\left(\frac{K_h}{P^0}\right) \right] \quad (14)$$

$$\Delta_{\text{sol}}S^{\infty} = \frac{(\Delta_{\text{sol}}H^{\infty} - \Delta_{\text{sol}}G^{\infty})}{T} \quad (15)$$

The pressure range considered in this work is not too high to cause Henry's law constant to be a strong function of pressure, and Henry's law is weakly dependent on pressure under the specified conditions. Therefore, it does not give rise to large errors if one ignores this pressure dependency. By means of this approximation and using eqs 13, 14, and 15, we estimated the thermodynamic functions of solution at infinite dilution for H<sub>2</sub>S and CO<sub>2</sub> in the IL. The values for the Gibbs energy, enthalpy, and entropy of solution are given in Table 3 for H<sub>2</sub>S and CO<sub>2</sub> in [hemim][BF<sub>4</sub>] at six discrete temperatures between (303.15 and 353.15) K. As it can be observed, the  $\Delta_{\text{sol}}G^{\infty}$  values are positive and increase with temperature in a similar manner for the solubility of both gases in IL. The  $\Delta_{\text{sol}}H^{\infty}$  values and  $\Delta_{\text{sol}}S^{\infty}$  values are negative. Because of strong hydrogen bonding interaction between the H<sub>2</sub>S and the hydroxyl group of the IL, the magnitudes of  $\Delta_{\text{sol}}H^{\infty}$  values are much greater for the solubility of H<sub>2</sub>S in the IL than they are in CO<sub>2</sub>. The variations with temperature of the  $\Delta_{\text{sol}}H^{\infty}$  values and  $\Delta_{\text{sol}}S^{\infty}$  values are positive for H<sub>2</sub>S and CO<sub>2</sub> in [hemim][BF<sub>4</sub>], and they increase with temperature.

As it was explained in the previous section, the diffusion measurements were made through the measurement of the variation of pressure with time from (2 to 20) min in which the magnetic stirrer was turned off. The pressure drop during the measurement of the diffusion coefficient varied from (0.23 to 0.22) MPa. The surface concentrations,  $C_{x=0}$ , of the solute (H<sub>2</sub>S or CO<sub>2</sub>) and the cumulative gas, which has diffused into semi-infinite volume at time  $t$ ,  $M_t$ , were calculated using the measured pressures at time  $t$  and the Henry's law constant. Figure 2 shows how  $C_{x=0}$  varies with the square root of time (eq 5), and Figure 3 shows the plot of  $M_t$  versus  $\varepsilon$ , where the diffusion coefficient was found from the slope squared (eq 7) for H<sub>2</sub>S in [hemim][BF<sub>4</sub>] at 303.15 K as an example. The diffusion coefficients calculated using the method described in the previous section are listed in Table 3. They were correlated with temperature using eq 16, and the obtained parameters  $C_i$  for H<sub>2</sub>S and CO<sub>2</sub> are summarized in Table 4.

$$(D/\text{cm}^2\cdot\text{s}^{-1}) = \sum_{i=0}^2 C_i(T/\text{K})^i \quad (16)$$

It can be observed that the diffusion coefficients of both gases in the IL increase with increasing temperature as long as the viscosity of the IL decreases. The diffusion coefficients of the two gases in the IL are approximately equal at about 313 K, and the difference between them increases by increasing the temperature. The van der Waals radii of both gases are approximately equal. Thus, the factor, which determines the diffusion coefficient of H<sub>2</sub>S to be larger than that of CO<sub>2</sub> in the IL at the lower temperature region, is the lower molecular weight

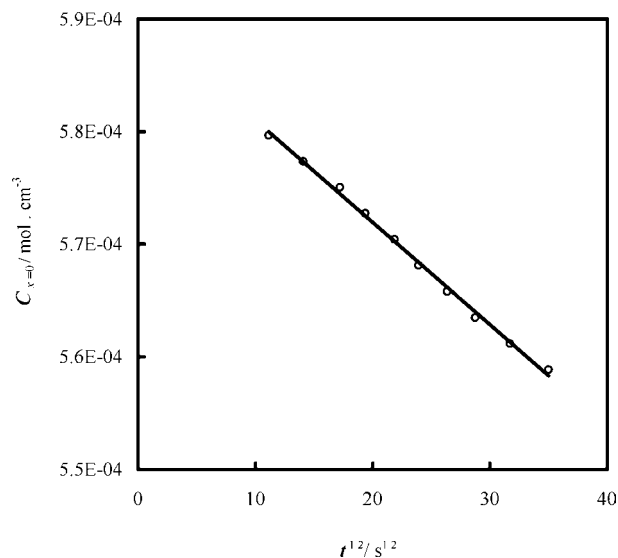


**Figure 2.** Surface concentration for H<sub>2</sub>S in [hemim][BF<sub>4</sub>] at 303.15 K as a function of the square root of time (eq 5).

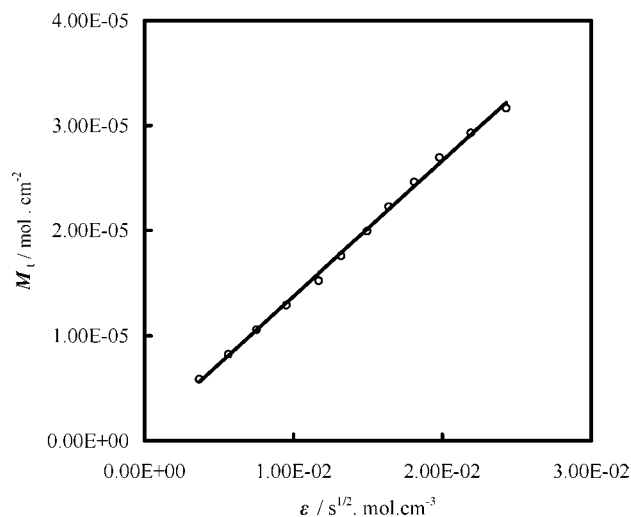


**Figure 3.** Plot of  $M_t$  versus  $\varepsilon = 2C_{x=0}(t/\pi)^{1/2} - (1/2)kt\pi^{1/2}$  for H<sub>2</sub>S in [hemim][BF<sub>4</sub>] at 303.15 K (eq 7).

of H<sub>2</sub>S relative to CO<sub>2</sub>. However, at higher temperatures the diffusion coefficient of H<sub>2</sub>S is lower than that of CO<sub>2</sub>. This behavior may be explained on the basis of the fact that as long as the force constant of the S—H bond in H<sub>2</sub>S (4.28 N·cm<sup>-1</sup>) is about four times lower than that of C=O bond in CO<sub>2</sub> (16 N·cm<sup>-1</sup>), the molecular size of H<sub>2</sub>S increases much more rapidly with temperature than that of CO<sub>2</sub>, which gives rise to the observed trend.

## Conclusion

New experimental data for the solubility, molar volume at infinite dilution, and diffusion coefficients of hydrogen sulfide and carbon dioxide gases in a functionalized IL [hemim][BF<sub>4</sub>] not previously reported in the literature have been measured and presented in this work. The solubility of carbon dioxide in [hemim][BF<sub>4</sub>] is lower than that of [emim][BF<sub>4</sub>], which is a conventional IL. The solubility of both gases in the IL studied in this work is of a physical nature. The solubility and diffusion coefficient of hydrogen sulfide in the IL are greater than those of carbon dioxide, indicating that this solvent can be used for the separation of these two gases from each other. The density of the IL at six temperatures was also reported, which indicates

that it is higher than that of corresponding IL, [emim][BF<sub>4</sub>], containing no hydroxyl functional group.

## Literature Cited

- (1) Kohl, A. L.; Nielsen, R. B. *Gas Purification*, 5th ed.; Gulf Publishing Company: Houston, TX, 1997.
- (2) Galán Sánchez, L. M.; Meindersma, G. W.; de Haan, A. B. Solvent Properties of Functionalized Ionic Liquids for CO<sub>2</sub> Absorption. *Chem. Eng. Res. Des.* **2007**, *85*, 31–39.
- (3) Wilkes, J. S. In *Ionic Liquids in Synthesis*; Wassercheid, P., Welton, T., Eds.; Wiley VCH: Verlag, 2002.
- (4) Bates, E. D.; Mayton, R. D.; Ntai, I.; Davis, J. H. CO<sub>2</sub> Capture by a Task-Specific Ionic Liquid. *J. Am. Chem. Soc.* **2002**, *124*, 926–927.
- (5) Shariati, A.; Peters, C. J. High-Pressure Phase Behavior of Systems with Ionic Liquids: II. The Binary System Carbon Dioxide + 1-Ethyl-3-methylimidazolium Hexafluorophosphate. *J. Supercrit. Fluids* **2004**, *29*, 43–48.
- (6) Camper, D.; Becker, C.; Koval, C.; Noble, R. Diffusion and Solubility Measurements in Room Temperature Ionic Liquids. *Ind. Eng. Chem. Res.* **2006**, *45*, 445–450.
- (7) Kroon, M. C.; Shariati, A.; Constantini, M.; van Spronsen, J.; Witkamp, G.-J.; Sheldon, R. A.; Peters, C. J. High-Pressure Phase Behavior of Systems with Ionic Liquids: Part V. The Binary System Carbon Dioxide + 1-Butyl-3-methylimidazolium Tetrafluoroborate. *J. Chem. Eng. Data* **2005**, *50*, 173–176.
- (8) Constantini, M.; Toussaint, V. A.; Shariati, A.; Peters, C. J.; Kikic, I. High Pressure Phase Behavior of Systems with Ionic Liquids. Part IV. Binary System Carbon Dioxide + 1-Hexyl-3-methylimidazolium Tetrafluoroborate. *J. Chem. Eng. Data* **2005**, *50*, 52–55.
- (9) Blanchard, L. A.; Gu, Z.; Brennecke, J. F. High Pressure Phase Behavior of Ionic Liquid/CO<sub>2</sub> Systems. *J. Phys. Chem. B* **2001**, *105*, 2437–2444.
- (10) Aki, S. N. V. K.; Mellein, B. R.; Saurer, E. M.; Brennecke, J. F. High-Pressure Phase Behavior of Carbon Dioxide with Imidazolium-Based Ionic Liquids. *J. Phys. Chem. B* **2004**, *108*, 20355–20365.
- (11) Jou, F.-Y.; Mather, A. E. Solubility of Hydrogen Sulfide in [bmim][PF<sub>6</sub>]. *Int. J. Thermophys.* **2007**, *28*, 490–495.
- (12) Pomelli, C. S.; Chiappe, C.; Vidis, A.; Laurency, G.; Dyson, P. J. Influence of the Interaction Between Hydrogen Sulfide and Ionic Liquids on Solubility: Experimental and Theoretical Investigation. *J. Phys. Chem. B* **2007**, *111*, 13014–13019.
- (13) Jalili, A. H.; Rahmati-Rostami, M.; Ghotbi, C.; Hosseini-Jenab, M.; Ahmadi, A. N. Solubility of H<sub>2</sub>S in Ionic Liquids [bmim][PF<sub>6</sub>], [bmim][BF<sub>4</sub>], and [bmim][Tf<sub>2</sub>N]. *J. Chem. Eng. Data* **2009**, *54*, 1844–1849.
- (14) Rahmati-Rostami, M.; Ghotbi, C.; Hosseini-Jenab, M.; Ahmadi, A. N.; Jalili, A. H. Solubility of H<sub>2</sub>S in Ionic Liquids [hmim][PF<sub>6</sub>], [hmim][BF<sub>4</sub>], and [hmim][Tf<sub>2</sub>N]. *J. Chem. Thermodyn.* **2009**, *41*, 1052–1055.
- (15) Yeon, S. H.; Kim, K. S.; Choi, S.; Lee, H. Physical and Electrochemical Properties of 1-(2-Hydroxyethyl)-3-methylimidazolium and N-(2-hydroxyethyl)-N-methyl morpholinium Ionic Liquids. *Electrochim. Acta* **2005**, *50*, 5399–5407.
- (16) Dubreuil, J. F.; Bazureau, J. P. Efficient Combination of Task-Specific Ionic Liquid and Microwave Dielectric Heating Applied to One-Pot Three Component Synthesis of a Small Library of 4-Thiazolidiones. *Tetrahedron* **2003**, *59*, 6121–6130.
- (17) NIST Scientific and Technical Databases, Thermophysical Properties of Fluid Systems. <http://webbook.nist.gov/chemistry/fluid/> (accessed May 2009).
- (18) Crank, J. *The Mathematics of Diffusion*, 2nd ed.; Clarendon Press: Oxford, U.K., 1979.
- (19) Bara, J. E.; Carlisle, T. K.; Gabriel, C. J.; Camper, D.; Finotello, A.; Gin, D. L.; Noble, R. D. Guide to CO<sub>2</sub> Separations in Imidazolium-Based Room-Temperature Ionic Liquids. *Ind. Eng. Chem. Res.* **2009**, *48*, 2739–2751.
- (20) Gardas, R. L.; Freire, M. G.; Carvalho, P. J.; Marrucho, I. M.; Fonseca, I. M. A.; Ferreira, A. G. M.; Coutinho, J. A. P. *P-ρ-T* Measurements of Imidazolium-Based Ionic Liquids. *J. Chem. Eng. Data* **2007**, *52*, 1881–1888.
- (21) Jacquemin, J.; Husson, P.; Majer, V.; Costa Gomes, M. F. Low-Pressure Solubilities and Thermodynamics of Solvation of Eight Gases in 1-Butyl-3-methylimidazolium Hexafluorophosphate. *Fluid Phase Equilib.* **2006**, *240*, 87–95.
- (22) Restolho, J.; Serro, A. P.; Mata, J. L.; Saramago, B. Viscosity and Surface Tension of 1-Ethanol-3-methylimidazolium Tetrafluoroborate and 1-Methyl-3-octylimidazolium Tetrafluoroborate over a Wide Temperature Range. *J. Chem. Eng. Data* **2009**, *54*, 950–955.

Received for review September 2, 2009. Accepted October 12, 2009. We are thankful to the research council of the Research Institute of Petroleum Industry (RIPI) and also to the Research and Development of the National Iranian Oil Company (NIOC) for their support of this work.

JE900716Q